

# Stability analysis of a river bank slope with an existing shear band

Rajib Dey & Bipul Hawlader

*Faculty of Engineering – Memorial University of Newfoundland, St. John's, Canada*

Ryan Phillips

*C-CORE, St. John's, Canada*

Kenichi Soga

*Faculty of Engineering – University of Cambridge, Cambridge, UK*

## ABSTRACT

Progressive failure of slopes near a river bank can cause large scale landslides. The presence of sensitive clay layers which show strain softening behaviour is considered as one of the main factors facilitating the progressive failure of such slopes. Various triggering factors such as river bank erosion, construction and other activities near the bank might initiate the failure of slopes. Once the movement is initiated in a small zone where sensitive clay layers exist, the imbalanced force is transferred to the surrounding soil in which slip surfaces might propagate in the form of a shear band through the sensitive clay layer. In this study, upward progressive failure due to river bank erosion has been modelled numerically incorporating nonlinear post-peak strain softening behaviour. Then the stability of this so-called stable slope, with an existing shear band in the sensitive clay layer, is further analysed for additional triggering loads. It is shown that additional loads from human activities near river banks such as embankment/road construction could cause a global failure of slopes with pre-existing shear bands. It is also shown that the brittleness of sensitive clay could accelerate the progressive failure of slopes.

## RÉSUMÉ

Défaillance progressive des pentes près d'une rivière peut provoquer des glissements de terrain à grande échelle. La présence de couches d'argile sensible qui présentent un comportement souche de ramollissement est considéré comme l'un des principaux facteurs favorisant la rupture progressive de ces pistes. Divers facteurs déclenchants tels que l'érosion des berges, la construction et d'autres activités à proximité de la banque pourraient engager l'échec des pistes. Une fois que le mouvement est initié dans une petite zone où les couches d'argile sensible existe, la force de déséquilibre est transférée vers le sol environnant dans lequel les surfaces de glissement peuvent se propager sous la forme d'une bande de cisaillement à travers la couche d'argile sensible. Dans cette étude, la rupture progressive à la hausse en raison de l'érosion des berges de la rivière a été modélisé numériquement intégrant le comportement post-pic souche de ramollissement non linéaire. Ensuite, la stabilité de cette pente dite stable, avec une bande de cisaillement existant dans la couche d'argile sensible, est en outre analysé pour déterminer les charges de déclenchement supplémentaires. Il est montré que les charges supplémentaires résultant des activités humaines à proximité des berges tels que la construction du remblai / route pourraient provoquer une panne mondiale de pistes avec des bandes de cisaillement préexistantes. Il est également montré que la fragilité de l'argile sensible pourrait accélérer la défaillance progressive des pentes.

## 1 INTRODUCTION

Large landslides in soft sensitive clays are common in Eastern Canada and Scandinavia and considered a major hazard in these countries because of their retrogressive potential and high mobility. Most onshore landslides which occurred in soft sensitive clay have been reported as progressive in nature (Bernander 2000, 2008, Locat et al. 2008, Quinn 2009, Locat et al. 2011, 2013). Progressive failure might be initiated in a fully stable and/or marginally stable slope depending on the nature of the triggering factors. Failure could propagate either in an upward or downward direction, towards the river bank, and the movement of the slope might be initiated because of the presence of a weak soil layer, where the shear stress is increased or soil strength is reduced by the triggering factors. The presence of strain-softening clay layers is one of the main reasons for progressive failure of a slope. These landslides could be in the form of multiple

retrogressive, translational progressive or spreads (Tavenas 1984, Karlsrud et al. 1984). Upward progressive failure might be initiated near river banks due to the presence of weak soil layers, where shear stress ratio is increased or soil strength is reduced by various triggering factors such as toe erosion. Large landslides in sensitive clays classified as spreads (Cruden and Varnes 1996) might be triggered by erosion near the toe of the river bank slope (Quinn et al. 2007, Locat et al. 2008). Numerous spread failures have been reported to be triggered by erosion at the toe of the slope (Bernander 2000, Locat et al. 2008, Quinn et al. 2007, Locat et al. 2011), although it is very difficult to identify the true disturbing agents which caused these spread failures. On the other hand, it has also been reported that additional applied loads or disturbance near the river bank due to human activities such as embankment construction, could cause disastrous landslides (for examples, the Svårta river slide, the Surte landslide in Sweden, the Tre-stycke

vattnet slide, and the Småröd slide) in a marginally stable or globally stable river bank slope if there is the presence of a sensitive clay deposit (Bernander 2000). Once this type of slide is initiated, the movement of the slide mass could constrict or completely block the river path, for example, as happened during the Surte landslide in Sweden. Triggering of these landslides in sensitive clay layers might be caused by a combination of both natural factors (e.g. toe erosion) and human activity (e.g. placement of fill) (L'Heureux et al. 2014). Therefore the failure might be a combination of both upward and downward progression in nature. The mechanisms of upward and downward progressive failure have been well documented in the literature (Bernander 2000, 2008, Locat et al. 2008, 2011).

Progressive failure might occur in drained as well as undrained conditions. Bjerrum (1967) explained drained upward progressive failure initiation in an intact slope containing overconsolidated plastic clays and clay shales. Sensitive clays from Eastern Canada and Scandinavia show strain softening behavior under undrained loading which has been considered as one of the main reasons for developing progressive failure (Bernander 2000, Locat et al. 2008, Quinn 2009, Locat et al. 2011). An undrained condition is considered in this study for analyzing progressive failure.

During the Ormen Lange field development, numerical simulations have been carried out by Norwegian Geotechnical Institute (NGI) using PLAXIS software to analyze the potential of retrogressive sliding due to strain softening effect in shallow clay slopes (NGI 2001). Anderson and Jostad (2007) conducted numerical analyses of progressive failure by modeling the shear band as an interface element using the NGI finite element (FE) code BIFURC. Quinn (2009) also demonstrated the use of linear elastic fracture mechanics concept in progressive failure of slopes. Recently, new numerical methods have been presented by Dey et al. (2013) to model the progressive failure of slopes with sensitive clay layers.

This paper uses the same numerical technique first published in Dey et al. (2013). This study initially describes how a small unloading event near the toe of the slope could cause local upward progressive failure in a sensitive clay deposit. Then it shows how a small triggering load due to human activities could trigger a downward progressive failure in this so-called stable slope and finally cause global failure of the slope due to combined triggering factors.

## 2 PROBLEM DEFINITION

The geometry of the slope used in the present FE modelling is shown in Figure 1. A 19 m high river bank slope is chosen for this study which has an angle of 30° with the horizontal. The ground surface is considered flat. The slope has two layers of soil above the strong base layer. A thick crust of strong clay is assumed near the face which overlies the 9 m high sensitive clay layer. For simplicity it is assumed that the groundwater table is at the crest of the slope and the river level is at the ground surface. The failure of this slope could also occur in

drained condition with no additional load; however, the focus of this study is to model the failure in undrained conditions under additional load. A triangular shape soil block near the toe of the slope shown by the hatched zone in Figure 1 is removed, which could be caused by erosion or by excavation during construction activities. This block will be referred as “excavated/eroded soil block.” The erosion of this block might cause upward progressive failure. In addition, downward progressive failure is modeled by later applying a vertical load on a rigid block located at 160 m from the crest of the slope. The width of the load block is 20 m. This load might come from various human activities such as construction of an embankment, stockpile of materials or other reasons. It is also assumed that the erosion and vertical loading from the load block occur relatively fast such that the deformation/failure of remaining soil occurs in undrained condition.

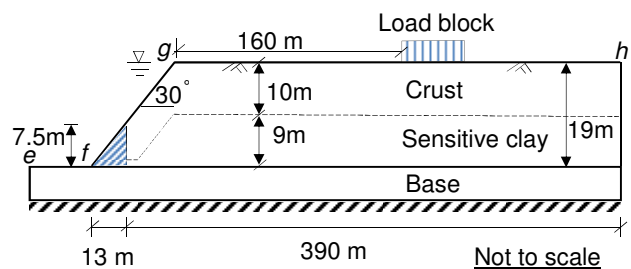


Figure 1. Geometry of the slope used in finite element modeling

Five different cases are analyzed in this study.

Case-1: Modeling of upward progressive failure is performed where toe erosion is assumed to be the triggering factor. The 9 m thick sensitive clay layer might exist in the field as a thin or thick layer. The thickness of the sensitive clay layer could affect the pattern of progressive failure as shown in Dey et al. (2013).

Case-2: Modeling of downward progressive failure is performed. A displacement-controlled load is applied at a distance of 160 m from the crest of the slope using the load block. No erosion of the toe of the slope is considered in this case.

Case-3: The combined effects of toe erosion and loading from the load block are investigated. The toe erosion is generated first. Then the vertical load is applied. The toe erosion causes upward progress of a shear band. The subsequent loading from the load block creates downward progress of other shear bands. The combined effects might result in global failure of the slope.

Case-4: The term “brittleness parameter” is used to model the rate of decrease of undrained shear strength with displacement, which is similar to Quinn et al. (2011). The effects of the brittleness parameter are examined in this case.

Case-5: The ground deformation or possible failure of the slope is analyzed when the clay layers are not sensitive. By comparing the results of this case with previous cases (1-4), it is shown how the sensitivity

changes the soil deformation pattern, formation of shear failure planes and the stability of the slope.

### 3 FINITE ELEMENT MODELING

#### 3.1 Numerical Technique

Abaqus 6.10 EF-1 is used in this study. The cases described above fundamentally involve large deformation as very significant plastic shear strain is developed in a thin layer of soil (also known as shear band) through which failure of the slope occurs. Conventional finite element techniques developed in a Lagrangian framework cannot model such large strain problems accurately because of significant mesh distortion. In order to overcome these issues, Coupled Eulerian-Lagrangian (CEL) technique currently available in Abaqus FE software is used. The finite element model consists of four parts: (i) soil, (ii) excavated/eroded soil block, (iii) rectangular load block to apply vertical load, and (iv) void space to accommodate the displaced soil mass. The soil is modeled as Eulerian material using EC3D8R elements, which are 8-noded linear brick, multi-material, reduced integration elements with hourglass control. In Abaqus CEL, the Eulerian material (soil) can flow through the fixed mesh. Therefore, there is no numerical issue of mesh distortion or mesh tangling even at very large strain in the zone around the failure plane.

The excavated/eroded soil block and load block are modeled in a Lagrangian framework as a rigid body, which makes the model computationally efficient. A void space is created above the model shown in Figure 1. Soil and void spaces are created in Eulerian domain using the Eulerian Volume Fraction (EVF) tool. For void space EVF is zero (i.e. no soil). On the other hand, EVF is unity in clay layers shown in Figure 1, which means these elements are filled with Eulerian material (soil).

Zero velocity boundary conditions are applied normal to the bottom and all the vertical faces (Figure 1) to make sure that Eulerian materials remain within the domain. That means, the bottom of the model shown in Figure 1 is restrained from movement in the vertical direction, while the vertical sides are restrained from any lateral movement. No boundary condition is applied at the soil-void interface (*efgh* in Figure 1).

Only three-dimensional models can be generated in the Abaqus CEL. In the present study, the model is only one element thick, which represents a plane strain condition.

The numerical analysis involved a number of steps. In the first step, geostatic load is applied to bring the soil to an in-situ condition. The slope is stable at the end of geostatic step with some shear stress, especially near the river bank. In the second step, the rigid excavated/eroded soil block is moved horizontally 750 mm to the left using displacement boundary condition except in Case-2. Finally, in third step the load block is moved vertically except in Case-1.

#### 3.2 Modeling of soil

Table 1 shows the geotechnical parameters used in this study. The crust has an undrained shear strength of 60

kPa, and a modulus of elasticity of 10 MPa ( $=167s_u$ ). The soil in the base layer is assumed to be very strong and hence only an elastic property,  $E_u=200$  MPa is considered.

Table 1. Parameters used in numerical modelling.

<u>Crust</u>	
Undrained modulus of elasticity, $E_u$ (kPa)	10,000
Undrained shear strength, $s_u$ (kPa)	60
Submerged unit weight of soil, $\gamma$ (kN/m <sup>3</sup> )	9.0
Poisson's ratio, $\nu_u$	0.499
<u>Sensitive clay</u>	
Undrained modulus of elasticity, $E_u$ (kPa)	7,500
Poisson's ratio, $\nu_u$	0.499
Peak undrained shear strength, $s_{up}$ (kPa)	50
Sensitivity, $S_t$	6
Submerged unit weight of soil, $\gamma$ (kN/m <sup>3</sup> )	8.0
Plastic shear strain for 95% degradation of soil strength, $\gamma_{95}^p$ (%)	25

#### 3.2.1 Modeling of stress softening behavior

Proper modeling of stress-strain behavior of sensitive clay layer is the key component of progressive failure analyses in sensitive clays. Sensitive clay shows post-peak softening behavior when it is subjected to undrained loading. Several authors (e.g. Tavenas et al. 1983, Quinn 2009) showed that the post-peak softening behavior is related to post-peak displacement or plastic shear strain. During any slope movement/failure in sensitive clays, shear deformation occurs along the thin layer of discontinuity (also known as shear band) that results in significant plastic shear strain. Brittleness of sensitive soils is one of the most important factors that controls the mobilized post-peak shear strength, especially in the zone of strain localization. Therefore, it is important to define the post-peak softening behavior properly. The following exponential relationship of shear strength degradation as a function of displacement is used in the present study.

$$s_u = [1 + (S_t - 1) \exp(-3\delta/\delta_{95})] s_{ur} \quad [1]$$

where  $s_u$  is the strain-softened undrained shear strength at  $\delta$ ;  $S_t$  is sensitivity of the soil;  $\delta = \delta_{total} - \delta_p$  where  $\delta_p$  is the displacement required to attain the peak undrained shear strength ( $s_{up}$ ); and  $\delta_{95}$  is the value of  $\delta$  at which the undrained shear strength of the soil is reduced by 95% of ( $s_{up} - s_{ur}$ ). Equation 1 is a modified form of strength degradation equation proposed by Einav and Randolph (2005) and was used by the authors (Dey et al. 2012, 2013) for modeling onshore and offshore slopes. If the thickness of shear band ( $t$ ) is known, the corresponding plastic shear strain ( $\gamma^p$ ) can be calculated

as,  $\gamma^p = \delta/t$  assuming simple shear condition. Therefore, Equation 1 in terms of  $\gamma^p$  can be written as

$$s_{ur} = [1 + (S_r - 1) \exp(-3\gamma^p / \gamma_{95}^p)] s_{ur} \quad [2]$$

where  $\gamma_{95}^p$  is the value of  $\gamma^p$  at 95% strength reduction (i.e.  $\gamma_{95}^p = \delta_{95}/t$ ). Note that, it is very difficult to determine the thickness of the shear band in the field. Similar to previous studies (e.g. Quinn 2009)  $t=0.5$  m is used which is same as the element height used in the present FE analysis. In the Abaqus FE software, the degradation of shear strength of sensitive clay is varied as a function of plastic strain. The parameters used to model the sensitive clay using Eq. 2 are also shown in Table 1. These parameters are estimated based on the laboratory tests conducted on sensitive clays (e.g. Tavenas et al. 1983) and the interpretation of test data and constitutive model development by other researchers (e.g. Bernander 2000, Leroueil 2001, Locat et al. 2008, Quinn 2009, Locat et al. 2011, and Locat et al. 2013).

## 4 FINITE ELEMENT RESULTS

### 4.1 Propagation of Shear Band

Figure 2 shows the generated equivalent plastic shear strain in Case-1 after the eroded soil block is moved to the left. In this case, the formation of the horizontal shear band is initiated along the sensitive clay layer just above the strong base when the movement of the excavated/eroded soil block is started. As the top soil mass is displaced due to the movement of eroded soil block, large plastic shear strain is generated in a thin layer of soil. The shear band propagates horizontally and finally ended with a length of 51.5 m when a gap is formed between the vertical face of eroded soil block and the soil mass at the right. Note that the shear band might go upward and cause slope failure depending on factors such as geometry of the slope, geotechnical properties of sensitive clay and amount of toe erosion as shown in Dey et al. (2013). However, no global failure occurred in this case as the released energy from the excavated/eroded soil block is insufficient. Also there is no sign of significant deformation at the ground surface.

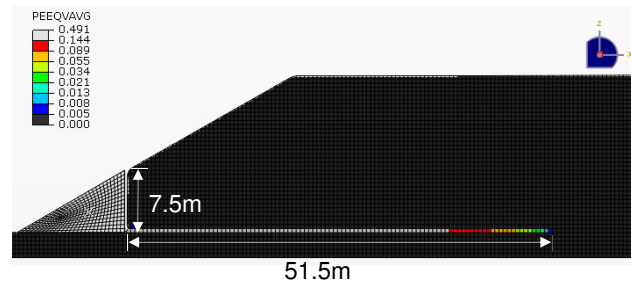


Figure 2. Equivalent plastic shear strain

The equivalent plastic shear strain, denoted by the symbol PEEQVAVG in Figure 2, is related to  $\gamma^p$  as  $PEEQVAVG = \gamma^p / \sqrt{3}$ . According to Eq. 2, when  $\gamma^p \geq \gamma_{95}^p$  ( $=0.25$ ), that means  $PEEQVAVG \geq 0.25 / \sqrt{3} = 0.144$ , the undrained shear strength is less than 10.4 kPa. The PEEQVAVG contour in Figure 2 shows that the generated shear band can be divided into two segments. The first segment, shown by the white color elements, covers almost 75% of the generated shear band in this case where the developed equivalent plastic shear strain is greater than 0.144. That means the soil elements in this section have shear strength less than 10.4 kPa ( $=s_{u95}$ ). The remaining 25% length of the generated shear band is known as “end zone” (colored section) where the shear strength gradually increases from  $s_{u95}$  to  $s_{up}$ .

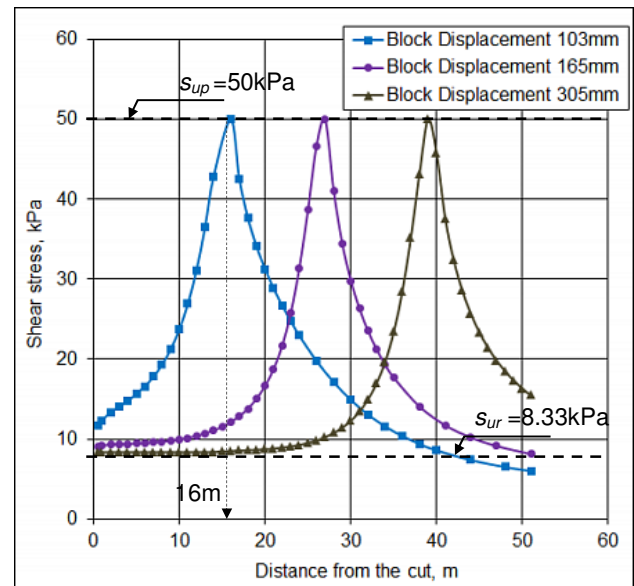


Figure 3. Variation of shear stress for different displacement of eroded block

### 4.2 Mobilized Shear Strength

Once the local failure is initiated in a small zone where sensitive clay layers exist, the imbalanced force is transferred to the surrounding soil in which the slip surface might propagate in the form of a shear band through the sensitive clay layer as shown in Figure 2. The progressive mobilization of shear strength along this shear band is explained in this section. Figure 3 shows the variation of shear stress along the failure plane with movement of excavated/eroded block for Case-1. The variation of shear stresses along the developed shear band is shown for three different block displacements (103 mm, 165 mm, and 305 mm). In order to explain the process, consider the shear stress on the potential failure plane for the block displacement of 103 mm. The maximum shear stress (50 kPa) is developed at 16 m from the vertical face of the cut. The shear stress between 0 to 16 m is less than 50 kPa (i.e.  $s_{up}$ ) and greater than

8.33 kPa (i.e.  $s_{ur}$ ). That means, 0-16 m of the shear band represents the post-peak softening zone where the reduction of shear strength occurred because of plastic strain as per Eq. 2, and the mobilized shear strength is in between the peak and residual shear strength of the soil. To the right side of the peak (i.e. distance greater than 16 m) the shear stress is again reduced with distance. For this displacement of the block (103 mm), the shear stress in this potential failure plane at a distance greater than 16 m has reached the peak, and therefore it represents the pre-peak behavior. At a very large distance, the shear stress is almost zero as the ground surface is horizontal. The pattern of shear stress development for other displacements of the block is similar as shown in Figure 3. The location of the peak shear stress shifts to the right with increase in block displacement; that means a greater length of the potential failure plane is in a post-peak stress-strain condition. For example, for 305 mm block movement the peak is at 39 m and therefore 0-39 m is in post-peak condition with approximately 20 m in residual shear strength level. This process will continue until the shear band propagation is ended for globally stable slopes as in Case-1.

## 5 COMPARISON WITH DIFFERENT CASES

In Case-1, it is shown that an upward progressive failure is initiated due to movement of the eroded soil block (Figure 2). A shear band propagates horizontally in to the soil and finally ends at a certain length. Therefore, the slope remains globally stable although it contains a 51.5 m long shear band. Toe erosion is the only triggering factor in this case. The generated shear band might propagate further and might result in global slope failure if; (i) additional triggering load is applied, (ii) quick degradation of soil shear strength occurs, or (iii) combination of both. The effects of these factors are discussed in the following sections.

### 5.1 Additional Triggering Load

To understand the effects of additional triggering load on slope stability, a displacement controlled load is applied vertically at a distance of 160 m from the point  $g$  in Figure 1. The rectangular load block is displaced vertically at a constant rate. Two cases are considered in this section. Figure 4 shows the FE results of Case-2 where only the displacement controlled load is applied. The following figures of this type are not to scale with the horizontal dimension reduced by a factor of 3. The slope is stable under gravity load and no shear band propagation occurs as no toe erosion is considered in this case. A triangular failure wedge is formed underneath the load block as expected as the load block is penetrated into the soil by an amount of approximately 200 mm (Figure 4a). At this stage, the vertical pressure on the soil from the load block is approximately 230 kPa. If the load block is pushed further, two shear bands are formed at both sides below the load block (Fig. 4b). Figure 4(b) shows the shear band formation at 790 mm movement of the block. It is shown later that soil pressure does not increase due to movement of the load block from 200 to 790 mm. In other

words, the ultimate capacity is reached at 200 mm displacement at a vertical pressure of 230 kPa. One interesting observation is that, shear band propagates horizontally through the sensitive clay layer due to the strain softening behavior of sensitive clay. In conclusion, although significant settlement of the load block occurred because of reduction of shear strength along the shear band, no global failure of the slope is calculated in this case.



Figure 4. Equivalent plastic shear strain in Case-2 for two vertical displacement of load block: a) 195 mm b) 790 mm

The combined effects of toe erosion and vertical loading (Case 3) are shown in Figure 5. As mentioned before in Case-3 the toe erosion is applied first, which creates a shear band of 51.5 m length as shown in Fig. 5(a). Therefore, the FE analysis in the third step for loading from the load block represents a downward progressive failure of a slope with a pre-existing shear band. Figures 5b to 5e show the shear band for four different vertical displacements of the load block. The propagation of shear bands started after a certain vertical displacement of the load block. There is a separation between the pre-existing shear band from toe erosion and the shear band formed by load block. For example, Figure 5b shows that there is a separation of 130.5 m when the load block is displaced vertically by an amount of 200 mm. As mentioned before, the ultimate capacity is reached at this stage. Further increase in load (pressure) will cause significant settlement. In the numerical analysis, vertical displacement is applied to the load block. The separation between the shear bands is reduced to 60.5 m as shown in Figure 5d when the load block is additionally displaced by 360 mm. Figure 5e shows that a complete failure surface is formed where shear strength drops almost to its residual value under a further 175 mm displacement. PEEQVAVG greater than 0.144 is generated along the whole shear band and finally causes global failure of the slope. The comparison of Figures 4(a) and 5(b) shows that the formation of a triangular wedge under the load block is similar in Case 2 and Case-3. For additional vertical displacement of the load block, the shear band in Case-3 is different from that in Case-2 (compare Figures 4(b) and 5c to 5e). In Case-3 there is a pre-existing shear band from toe erosion where the shear strength is reduced almost to the residual value. As the resistance is reduced, the soil block in the left side

of the load block has more freedom to move leftward. This creates another triangular wedge and the soil mainly moves to the left. When sufficient leftward movement occurred, the shear band in the right side of the load block starts to grow as shown in 5(d). This is very different from Case-2 where the shear bands are almost symmetric under the load block. The FE analysis of this case shows that the existence of a shear band in the strain softening clay layer in a so-called globally stable slope could cause a massive slope failure if there are some human activities that create sufficient vertical load at a certain distance from the slope. This might even come from temporary works such as stockpile of materials. Moreover, the combined effects of two triggering factors cause the global failure in Case-3, while global failure is not caused either in Case-1 or Case-2 with single triggering factor for the assumed conditions.

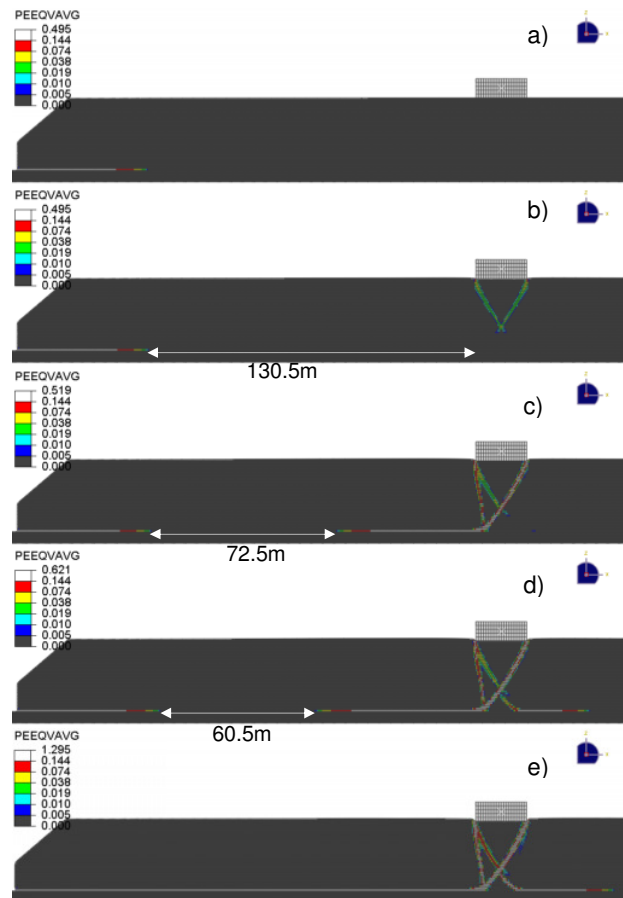


Figure 5. Position of shear band in Case-3 for different vertical displacement of load block; a) zero mm, b) 200 mm, c) 460 mm, d) 560 mm, e) 735 mm

## 5.2 Effect of Strain Softening Curve

Strain softening behavior is considered one of the most important properties of sensitive clay. Besides sensitivity, the value of  $\delta_{95}$  or  $\gamma_{95}^p$  controls the strain softening behavior of sensitive clay as shown in Eq. 1 or Eq. 2. In this study, the clay sensitivity is kept constant, however

two different values of  $\delta_{95}$  are considered as shown in Figure 6. The upper line in Fig. 6 is less brittle than the lower one. The analyses presented in the previous sections are based on the upper line. To show the effects on brittleness, Case-3 is analysed again using the lower curve in Figure 6, where the  $\delta_{95}=90$  mm is used. The shear band formation for this soil parameter is shown in Figure 7. The length of the shear band due to toe erosion is increased to 63.5 m (Fig. 7a) which was 51.5 m with the lower brittleness value (Fig. 5a). Similar to Fig. 5(b), a triangular wedge is formed due to the vertical displacement of the load block (Fig. 7b). However, the global failure occurred at 450 mm of vertical displacement of the load block (Fig. 7d), which is lower than the value presented in Fig. 5. In other words, the brittleness of shear strength curve (Fig. 6) has significant effects on shear band formation and failure of the slope.

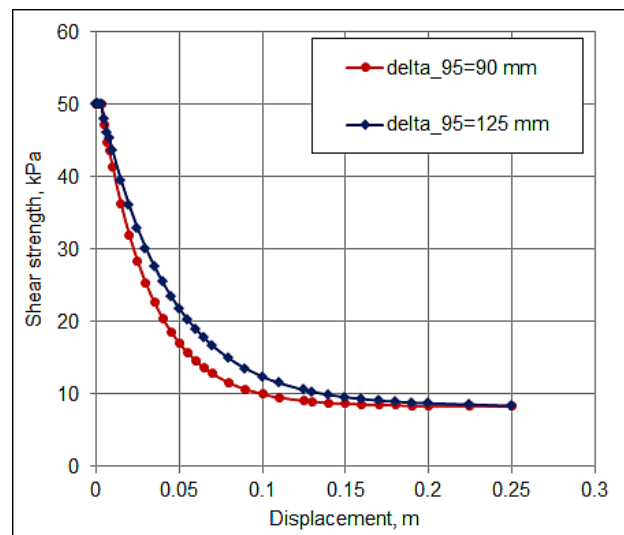


Figure 6. Variation of strain softening curve

To understand softening effects on deformation/failure mechanism, Case-4 is reanalyzed without any softening. That means, the soil is simply modeled as elasto-plastic material of undrained shear strength  $s_u=50$  kPa. Figure 8(a) shows that plastic shear strain is developed in a small zone of soil due to toe erosion. During vertical movement of the load block, a triangular wedge is formed at a vertical displacement of 235 mm. If the displacement is continued, local shear failure type slip surfaces are generated at a vertical displacement of 900 mm (Figure 8c).

## 5.3 Pressure under load block

Vertical displacement is applied to the load block to simulate the loading. Average pressures developed below the load block due to applied vertical displacement for the different cases are shown in Figure 9. A triangular failure wedge is initially developed in all cases at an approximate displacement of 200 mm.

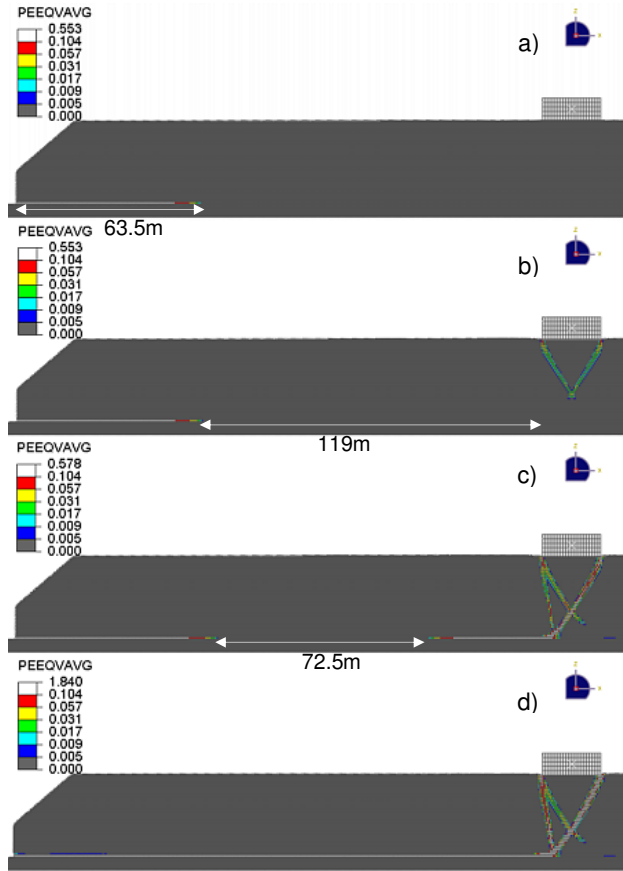


Figure 7. Shear band in Case-4 for four vertical displacement of load block: a) zero mm, b) 185 mm, c) 310 mm, d) 450 mm

The load displacement curve in Figure 9 is almost the same up to 200 mm displacement for all cases. However, the pressure starts to drop with further displacement in Cases 2-4 where strain depended softening is used. On the contrary, in Case-5 the average pressure continuously increases with displacement as no softening is considered in this case. The rate of decrease of vertical pressure in Case 4 is higher than that of in Cases 2 and 3, because of faster degradation of shear strength. The pressure decreases significantly in Cases 3 and 4 at vertical displacement of load block of 715 mm and 435 mm, respectively. Both of these cases contain a pre-existing shear band due to toe erosion. When the shear band generated due to downward movement of the load block merges with the pre-existing shear band, a complete failure surface is developed and the slope starts to move towards the river and global failure of the slope occurs. Approximately 280 mm less vertical displacement of the load block is required to cause global failure of the slope when the value of  $\delta_{95}$  is reduced to 90 mm (Case-4) from 125 mm (Case-3). On contrary, no such drop is calculated in Case-2 because the global failure of the slope does not occur. However, if the applied pressure is more than 230 kPa, a very large settlement will occur and result in punching failure.

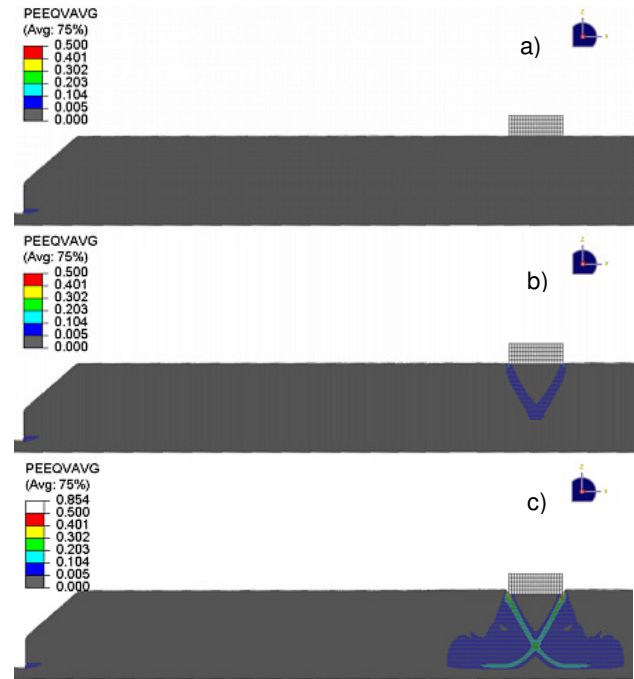


Figure 8. Plastic shear strain in Case-5; a) after toe erosion, b) at 235 mm, & c) at 900 mm vertical displacement of the rectangular block

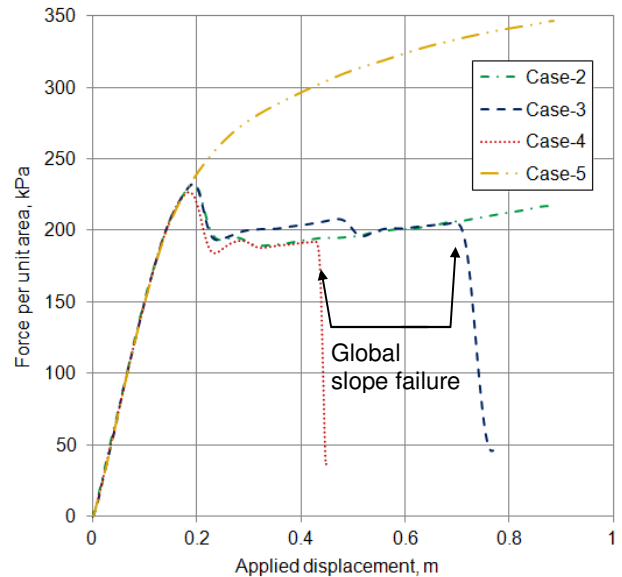


Figure 9. Comparison on force-displacement plot among Case-2 to Case-5

## 6 CONCLUSIONS

A new numerical approach to model the initiation and propagation of shear bands in both upward and downward progressive failure, as might be encountered near river banks comprising sensitive clays, is presented in this paper. The numerical technique of modeling progressive failure using Coupled Eulerian-Lagrangian (CEL) approach currently available in Abaqus FE software is first introduced by the authors in Dey et al. (2013). Nonlinear strain softening behavior of sensitive clay is incorporated in this large deformation finite element analysis. Five cases are analyzed in this study. Toe erosion is considered as an initial triggering factor and a displacement controlled load is applied as additional triggering factor. Additional triggering load from human activities such as embankment construction could cause a disastrous slope failure in Cases-3 and 4 due to presence of an existing shear band generated from toe erosion. Failure could be accelerated (fails at lower additional triggering load) if the brittleness of the sensitive clay is comparatively higher.

## ACKNOWLEDGEMENTS

The writers would like to acknowledge the financial support from Research & Development Corporation of Newfoundland and Labrador, NSERC and C-CORE.

## REFERENCES

- Anderson, L. and Jostad, H.P. 2007. Numerical modeling of failure mechanisms in sensitive soft clays — application to offshore geohazards. *Offshore Technology Conference*, Texas. Paper OTC 18650.
- Bernander, S. 2000. Progressive failure in long natural slopes: formation, potential extension and configuration of finished slides in strain-softening soils. Licentiate Thesis, Luleå University of Technology.
- Bernander, S. 2008. Down-hill progressive landslides in soft clays, triggering disturbance agents, slide propagation over horizontal or gently sloping ground, sensitivity related to geometry. Luleå University of Technology, Luleå, Sweden. Research report.
- Bjerrum, L. 1967. Progressive failure in slopes in overconsolidated plastic clay and clay shales. Terzaghi Lecture. *Journal of the Soil Mechanics and Foundation Division*, ASCE, 93(5): 3-49.
- Cruden, D.M. and Varnes, D.J. 1996. Landslides types and processes. In *Landslides investigation and mitigation. Special Report 247*. Transportation Research Board, NRC. Edited by A.K. Turner and R.L. Schuster. National Academy Press, Washington, D.C., 37-75.
- Dey, R., Hawlader, B., Phillips, R. and Soga, K. 2012. Effects of shear band propagation on submarine landslide. *Proc. of the 22<sup>nd</sup> Int. Offshore and Polar Engineering Conf.*, Rhodes, Greece, 766- 773.
- Dey, R., Hawlader, B., Phillips, R. and Soga, K. 2013. Progressive failure of slopes with sensitive clay layers. *Proc. of the 18<sup>th</sup> Int. Conference on Soil Mechanics and Geotechnical Engineering*, Paris.
- Einav, I. and Randolph, M.F. 2005. Combining upper bound and strain path methods for evaluating penetration resistance. *Int. Journal Numerical Methods Engineering*, 63(14): 1991-2016.
- Karlsrud, K., Aas, G. and Gregersen, O. 1984. Can we predict landslide hazards in soft sensitive clays? Summary of Norwegian practice and experiences. In *Proc. of the 4th Int. Symposium on Landslides*, Toronto, Ont., 1:107-130.
- L'Heureux, J.S., Locat, A., Leroueil, S., Demers, D. and Locat, J. 2014. *Landslides in sensitive clays: From geosciences to risk management*, 2nd ed., Springer, Dordrecht, Netherlands.
- Leroueil, S. 2001. Natural slopes and cuts: movement and failure mechanisms. *Géotechnique*, 51(3): 197-243.
- Locat, A., Leroueil, S., Bernander, S., Demers, D., Locat, J. and Ouehb, L. 2008. Study of a lateral spread failure in an eastern Canada clay deposit in relation with progressive failure: the Saint-Barnabé-Nord slide. In *Proc. of the 4th Canadian Conf. on Geohazards: From Causes to Management*, Québec, Que., 89-96.
- Locat, A., Leroueil, S., Bernander, S., Demers, D., Jostad, H.P. and Ouehb, L. 2011. Progressive failures in eastern Canadian and Scandinavian sensitive clays. *Canadian Geotechnical Journal*, 48(11): 1696-1712.
- Locat, A., Jostad, H.P. and Leroueil, S. 2013. Numerical modeling of progressive failure and its implications for spreads in sensitive clays. *Canadian Geotechnical Journal*, 50: 961-978.
- NGI Report 2001. Effect of strain softening on stability analysis. Analysis of retrogressive sliding due to strain softening-Ormen Lange case study, Report No 521001 (10).
- Quinn, P., Diederichs, M.S., Hutchinson, D.J. and Rowe, R.K. 2007. An exploration of the mechanics of retrogressive landslides in sensitive clay. In *Proc. of the 60th Canadian Geotechnical Conf.*, Ottawa, Ontario, 721-727.
- Quinn, P. 2009. Large Landslides in Sensitive Clay in Eastern Canada and the Associated Hazard and Risk to Linear Infrastructure. Doctoral thesis, Queen's University.
- Tavenas, F., Flon, P., Leroueil, S. and Lebus, J. 1983. Remolding energy and risk of slide retrogression in sensitive clays. *Proc. of the Symposium on Slopes on Soft Clays*, Linköping, Sweden, SGI Report No. 17: 423-454.
- Tavenas, F. 1984. Landslides in Canadian sensitive clays — a state-of-the-art. In *Proc. of the 4th Int. Symposium on Landslides*, Toronto, Ont., 1:141-153.